

# On Convergence of Certain Finite Volume Difference Discretizations for 1D Poroelasticity Interface Problems

Richard E. Ewing,<sup>1</sup> Oleg P. Iliev,<sup>2</sup> Raytcho D. Lazarov,<sup>3</sup> Anna Naumovich<sup>4</sup>

<sup>1</sup>*Institute for Scientific Computing, Texas A&M University, College Station, TX 77843*

<sup>2</sup>*Fraunhofer Institut fuer Techno- und Wirtschaftsmathematik, 67663 Kaiserslautern, Germany*

<sup>3</sup>*Department of Mathematics, Texas A&M University, College Station, TX 77843*

<sup>4</sup>*Fraunhofer Institut fuer Techno- und Wirtschaftsmathematik, 67663 Kaiserslautern, Germany*

*Received 28 February 2006; accepted 9 July 2006*

*Published online 16 November 2006 in Wiley InterScience (www.interscience.wiley.com).*

*DOI 10.1002/num.20184*

In the article two finite difference schemes for the 1D poroelasticity equations (Biot model) with discontinuous coefficients are derived, analyzed, and numerically tested. A recent discretization [Gaspar et al., *Appl Numer Math* 44 (2003), 487–506] of these equations with constant coefficients on a staggered grid is used as a basis. Special attention is given to the interfaces and as a result a scheme with harmonic averaging of the coefficients is derived. Convergence rate of  $O(h^{3/2})$  in a discrete  $H^1$ -norm for both the pressure and the displacement is established in the case of an arbitrary position of the interface. Further, rate of  $O(h^2)$  is proven for the case when the interface coincides with a grid node. Following an approach applied to second-order elliptic equations in [Ewing et al., *SIAM J Sci Comp* 23(4) (2001), 1334–1350] we derive a modified and more accurate discretization that gives second-order convergence of the fluid velocity and the stress of the solid. Finally, numerical experiments of model problems that confirm the theoretical considerations are presented. © 2006 Wiley Periodicals, Inc. *Numer Methods Partial Differential Eq* 23: 652–671, 2007

*Keywords:* finite differences; harmonic averaging; poroelasticity; multilayered media; interface problem; error analysis

## 1. INTRODUCTION

The classical Biot model treats consolidation of linearly elastic porous solid in a bounded domain  $\Omega \subset R^d$  with boundary  $\Gamma$ , which is either fully saturated by a slightly compressible fluid, or is

*Correspondence to:* Richard E. Ewing, Institute for Scientific Computing, Texas A&M University, College Station, TX 77843 (email: ewing@math.tamu.edu)

Contract grant sponsor: INTAS project; contract grant number: 03-50-4395

Contract grant sponsor: Kaiserslautern Excellence Cluster Dependable Adaptive Systems and Mathematical Modelling

Contract grant sponsor: National Science Foundation, EIA; contract grant number: 0218229 (to R.E.E and R.D.L.)

*Mathematics Subject Classification:* primary 65N15; 65N30; 76D07; secondary 35B45, 35J50

© 2006 Wiley Periodicals, Inc.

almost saturated with incompressible fluid. The fluid pressure  $p(x, t)$  and the displacement of the media  $\mathbf{u} = (u_1, \dots, u_d)$  satisfy the following system:

$$-\nabla \cdot \boldsymbol{\sigma} + \alpha \nabla p = \mathbf{h}(x, t), \quad (1)$$

$$\frac{\partial}{\partial t} (\phi \beta p + \alpha \nabla \cdot \mathbf{u}) - \nabla \cdot \left( \frac{k}{\eta} \nabla p \right) = f(x, t), \quad (2)$$

consisting of the equilibrium equation for the momentum and the diffusion equation for the Darcy flow. Here  $\phi$  is the porosity,  $\beta$  is compressibility of the fluid,  $k > 0$  is the permeability, and  $\eta$  the viscosity of the fluid as a measure of the Darcy flow corresponding to a pressure gradient. The term  $\alpha \nabla p$  in the first equation results from the additional stress of the fluid pressure within the structure and  $\alpha \nabla \cdot \mathbf{u}$  in the second equation represents the additional fluid content due to local volume change. Constant  $\alpha$ , called Biot's constant, accounts for the deformability of the grains of the porous material. Further we assume that the granular material itself is incompressible, which results in  $\alpha = 1$ . Stress tensor  $\boldsymbol{\sigma} = \boldsymbol{\sigma}(\mathbf{u})$  in the first equation is a symmetric  $d \times d$  tensor with components  $\sigma_{ij}$ ,  $i, j = 1, \dots, d$ , which is related to the small strain tensor  $\boldsymbol{\varepsilon} = \boldsymbol{\varepsilon}(\mathbf{u})$  with components  $\varepsilon_{ij} = \frac{1}{2}(\partial u_i / \partial x_j + \partial u_j / \partial x_i)$ ,  $i, j = 1, \dots, d$  via the linear stress-strain relations (Hook's law)  $\sigma_{ij} = 2\mu \varepsilon_{ij} + \lambda \nabla \cdot \mathbf{u} \delta_{ij}$ ,  $i, j = 1, \dots, d$ . Here  $\mu = \mu(x) > 0$  (shear moduli) and  $\lambda = \lambda(x) > 0$  (dilation moduli) are the Lamé coefficients of the elastic media (in general piecewise smooth functions, e.g., piecewise constants). Above  $\nabla \cdot \boldsymbol{\sigma}$  denotes a vector with  $i$ th component  $\sum_{j=1}^d \partial \sigma_{ij} / \partial x_j$ . This system is supplied with relevant boundary conditions that have clear physical meaning. For example, the pressure  $p = g$  could be prescribed on part of the boundary  $\Gamma_D$  and "no-flow" condition  $k \nabla p \cdot \mathbf{n} = 0$  on the rest of the boundary  $\Gamma_N$ . Here  $\mathbf{n}$  is the unit normal vector to  $\Gamma$ , pointing outside the domain  $\Omega$ . For the displacement we may have  $\mathbf{u} = 0$  on  $\Gamma_0$  and  $\boldsymbol{\sigma} \cdot \mathbf{n} = \mathbf{g}$  on  $\Gamma_t$  that corresponds to the case when the elastic body is clamped on  $\Gamma_0$  and have prescribed traction force on  $\Gamma_t$ .

This system is remarkable in many respects. First, it is a good approximation of a physical process for which the deformations vary sufficiently slowly so that the inertia effects are negligible. Second, it is a reasonable simplification of more general system of partially saturated porous media of barotropic fluids with density  $\rho = \rho(p)$ , a model that involves as an additional variable the saturation  $S$  and one additional equation. This and other models are important tools in simulations of flow in porous media and have numerous engineering applications.

The Biot model [1] (see also [2, 3] and references therein) describes well a class of fluid flows in deformable porous media, which is of interest for geosciences, bioscience, and engineering. Analysis of the well-posedness, uniqueness, and existence of the solution of this problem can be found, for example, in [4].

Solutions of Biot system in closed form is available only in very special cases see, e.g. [5, 6]. Therefore, numerical methods are commonly used for solving the respective initial-boundary value problem. The finite element method is preferred in many cases, especially when dealing with complex domains or adaptive grids (see, e.g., [3, 7, 8]). However, often solutions generated by finite elements and finite differences on collocated grids exhibit nonphysical oscillations at the early stages of the time stepping (i.e., close to the initial state). To avoid this difficulty certain discretization on staggered grid have been suggested and theoretically analyzed in [9, 10] in the case when the coefficients of the poroelasticity system are smooth. The situation is quite complicated when the coefficients have discontinuities along material interfaces, e.g., multilayered porous media, especially when it is essential to capture accurately the solution near the interface.

A finite difference scheme for multilayered porous domain has been developed in [11] and a number of numerical experiments have been presented and discussed. The scheme in [11] uses

staggered grids for the pressure  $p$  and the displacement  $u$  and approximation of the fluxes and stresses with harmonic averaging of the coefficients. Such an approach for second-order elliptic equations has been developed in the 1960s by Samarskii and is summarized in his monograph [12, Chapter 3]. One of the goals of this article is to analyze the schemes from [11] in the case of discontinuous coefficients. In Section 4 we show  $O(h^{3/2})$ -rate of convergence in an operator norm equivalent to the “energy norm” for arbitrary locations of the interfaces and  $O(h^2)$ -rate, when the interfaces coincide with grid nodes associated with displacements. Further, following the approach developed earlier in [13] for a scalar elliptic equation with discontinuous coefficients, we derive a modified and more accurate variant of this scheme (called modified scheme with harmonic averaging of the coefficients).

The remainder of the article is organized as follows. The Biot model, describing poroelasticity of a multilayered porous media, and its finite difference discretization are presented in Section 2. Section 3 is devoted to convergence analysis of the scheme using harmonic averaging. Since the proofs are very technical, we have moved them to an Appendix. Section 4 contains derivation of modified finite volume difference schemes that use the equations to improve the approximation near the interface. Finally, in Section 5 numerical experiments on several model problems are given and some conclusions are drawn.

## 2. PROBLEM FORMULATION AND ITS FINITE DIFFERENCE APPROXIMATION

### 2.1. Continuous Problem

In this article we consider an one-dimensional (1D) Biot model (1), (2) with discontinuous coefficients. We assume no external bulk forces are acting on the porous media so that the first equation is homogeneous, i.e.,  $h(x, t) = 0$ . For the full formulation of the problem with boundary conditions and a special choice of the initial conditions, we refer to [9].

First we introduce dimensionless dependent and independent functions by using the characteristic length, and reference values for the permeability, Lamé coefficients, etc. (see, e.g., [9]). Our focus is on the accurate treatment of the interface condition. In order to simplify the exposition we shall assume that the coefficients are discontinuous at just one interface point  $\zeta \in (0, 1)$ . Thus, we consider the following 1D variant of (1), (2):

$$\begin{aligned} -\frac{\partial}{\partial x} \left( v \frac{\partial u}{\partial x} \right) + \frac{\partial p}{\partial x} &= 0, & x \in (0, 1), \quad t \in (0, T], \\ \frac{\partial}{\partial t} \left( ap + \frac{\partial u}{\partial x} \right) - \frac{\partial}{\partial x} \left( k \frac{\partial p}{\partial x} \right) &= f(x, t), & x \in (0, 1), \quad t \in (0, T], \\ v \frac{\partial u}{\partial x} &= 0, \quad p = 0, & \text{if } x = 0, \quad t \in [0, T], \\ u = 0, \quad k \frac{\partial p}{\partial x} &= 0, & \text{if } x = 1, \quad t \in [0, T], \\ ap + \frac{\partial u}{\partial x} &= 1, & \text{if } t = 0, \quad x \in (0, 1), \\ [u] = 0, \quad \left[ v \frac{\partial u}{\partial x} \right] &= 0, \quad [p] = 0, \quad \left[ k \frac{\partial p}{\partial x} \right] = 0, & \text{for } x = \zeta, \quad t \in [0, T]. \end{aligned} \quad (3)$$

So-called consistent initial conditions are used at  $t = 0$  above (for more details see discussion and references in [9]). Here  $[g]$  denotes the jump  $g$  at the interface point  $\zeta$ . Also, we have used the notations for the dimensionless coefficients  $\nu(x) = (\lambda + 2\mu)/(\lambda_0 + 2\mu_0)$ ,  $a(x) = \phi\beta(\lambda_0 + 2\mu_0)$ , and  $k(x)$  replaced by  $k(x)/k_0$ , where  $\lambda_0$ ,  $\mu_0$ , and  $k_0$  are some reference values. Further, to distinguish the possible discontinuity of the coefficients at  $x = \zeta$ , we use the notations

$$\nu(x) = \begin{cases} \nu_1(x) & x < \zeta, \\ \nu_2(x) & x > \zeta, \end{cases} \quad a(x) = \begin{cases} a_1(x) & x < \zeta, \\ a_2(x) & x > \zeta, \end{cases} \quad k(x) = \begin{cases} k_1(x) & x < \zeta, \\ k_2(x) & x > \zeta. \end{cases} \quad (4)$$

**2.2. Grids and Notations for Finite Differences and Discrete Norms**

We split the interval  $(0, 1)$  into  $N > 1$  equal subintervals of size  $h = 2/(2N - 1)$ . We use two different spatial grids (so-called staggered grids),  $\bar{\omega}_p$  to discretize the pressure equation, and  $\bar{\omega}_u$  to discretize the displacement equation, and a grid in time  $t$  with a step-size  $\tau$ :

$$\begin{aligned} \bar{\omega}_p &= \{x_i : x_i = ih, i = 0, \dots, N - 1\}, & \omega_p &= \{x_i \in \bar{\omega}_p, i = 1, \dots, N - 1\}, \\ \bar{\omega}_u &= \{\xi_i : \xi_i = x_i - 0.5h, i = 1, \dots, N\}, & \omega_u &= \{\xi_i \in \bar{\omega}_u, i = 1, \dots, N - 1\}, \\ \omega_T &= \{t_j : t_j = j\tau, j = 1, 2, \dots, M\}. \end{aligned} \quad (5)$$

One may look at these meshes as designed to represent the values of the pressure  $p$  at the grid points  $x_i \in \bar{\omega}_p$  and the values of the displacement  $u$  at the midpoints  $\xi_i \in \bar{\omega}_u$  of the subintervals  $(x_{i-1}, x_i)$  (see Fig. 1). The position of the interface  $\zeta$  could be represented in the form

$$\zeta = \xi_n + \theta h, \quad (6)$$

where  $0 < n < N$  is an integer and  $0 \leq \theta < 1$ .

Now we shall introduce the following shorthand notations for discrete functions defined on  $\bar{\omega}_p \times \omega_T$  and  $\bar{\omega}_u \times \omega_T$ , respectively:

$$\begin{aligned} u &:= u^j := u_i^j := u(\xi_i, t_j), & p &:= p^j := p_i^j := p(x_i, t_j), \\ & & v^\sigma &:= \sigma v^{j+1} + (1 - \sigma)v^j, & \hat{v} &:= v^{j+1}. \end{aligned}$$

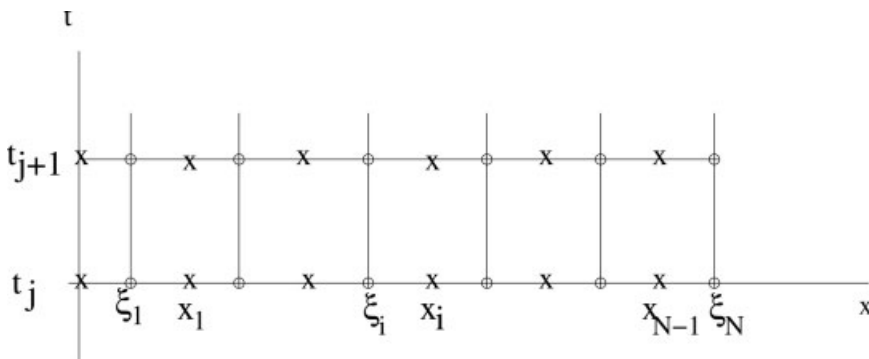


FIG. 1. Meshes: o, mesh points of  $\omega_u$ ; X, mesh points of  $\omega_p$ .

We introduce Hilbert space  $H_{\bar{\omega}_p}$  of discrete functions  $p = (p_0, p_1, \dots, p_{N-1})$  defined on the grid  $\bar{\omega}_p$  and Hilbert space  $H_{\bar{\omega}_u}$  of functions  $u = (u_1, u_2, \dots, u_N)$  defined on the grid  $\bar{\omega}_u$ . The respective inner products and norms in these spaces are

$$(p, q)_{\bar{\omega}_p} = \sum_{i=0}^{N-1} hp_i q_i, \quad \|p\|_{\bar{\omega}_p} = (p, p)_{\bar{\omega}_p}^{1/2}, \quad (u, v)_{\bar{\omega}_u} = \sum_{i=1}^N hu_i v_i, \quad \|u\|_{\bar{\omega}_u} = (u, u)_{\bar{\omega}_u}^{1/2}.$$

We also introduce Hilbert spaces  $H_{\omega_p}$  and  $H_{\omega_u}$  of grid functions  $p = (p_1, p_2, \dots, p_{N-1})$  and  $u = (u_1, u_2, \dots, u_{N-1})$  defined on the grids  $\omega_p$  and  $\omega_u$ , respectively, with following inner products and norms:

$$(p, q)_{\omega_p} = \sum_{i=1}^{N-1} hp_i q_i, \quad \|p\|_{\omega_p} = (p, p)_{\omega_p}^{1/2}, \quad (u, v)_{\omega_u} = \sum_{i=1}^{N-1} hu_i v_i, \quad \|u\|_{\omega_u} = (u, u)_{\omega_u}^{1/2}.$$

Further, we shall use the standard notation for the first-order backward and forward finite differences on a uniform mesh (see, e.g., [12]):

$$p_x := p_{x,i} = (p(x_{i+1}) - p(x_i))/h, \quad p_{\bar{x}} := p_{\bar{x},i} = (p(x_i) - p(x_{i-1}))/h.$$

Inspecting these expressions, we see that they represent central differences with respect to the points in  $\omega_u$ , and therefore we can consider them as quantities defined on the mesh  $\omega_u$ . In a similar way we define

$$u_x := u_{x,i} = (u(\xi_{i+1}) - u(\xi_i))/h, \quad u_{\bar{x}} := u_{\bar{x},i} = (u(\xi_i) - u(\xi_{i-1}))/h,$$

which represent central differences with respect to the points in  $\omega_p$  and could be considered as quantities defined on the mesh  $\omega_p$ . Finally, we define the finite differences in time

$$u_t := u_t^j := u_t(\xi_i, t_j) = (u_i^{j+1} - u_i^j)/\tau, \quad \xi_i \in \omega_u, \\ p_t := p_t^j := p_t(x_i, t_j) = (p_i^{j+1} - p_i^j)/\tau, \quad x_i \in \omega_p.$$

### 2.3. Finite Difference Scheme

We approximate the differential problem (3) by finite volume method. We integrate the first equation over each interval  $(x_{i-1}, x_i)$  and the second equation on  $(\xi_i, \xi_{i+1})$ . To approximate the quantities  $W(x_i) := \nu(\partial u/\partial x)(x_i)$  and  $V(\xi_i) := -k(\partial p/\partial x)(\xi_i)$  we look at  $W(x)$  and  $V(x)$  as new dependent “flux” variables solve for  $\partial u/\partial x$  and  $\partial p/\partial x$  and integrate over the meshes  $\omega_u$  and  $\omega_p$  to get the harmonic averaging of  $\nu$  and  $k$  expressed in (8). For more details we refer to [12, Chapter 3, pp 150–155] or [13]. Then choosing an implicit discretization in time we get the following finite difference scheme for the discrete approximate solution  $u = u_i^j$  at point  $(\xi_i, t_j) \in \omega_u \times \omega_T$  and  $p = p_i^j$  at grid point  $(x_i, t_j) \in \omega_p \times \omega_T$ :

$$-\frac{\nu}{h}\hat{u}_x + \hat{p}_{\bar{x}} = 0, \quad \xi = \xi_1, \quad t \in \omega_T \quad (i.e. i = 1), \\ -(v\hat{u}_{\bar{x}})_x + \hat{p}_{\bar{x}} = 0, \quad \xi = \xi_i \in \omega_u \setminus \{\xi_1\}, \quad t \in \omega_T \quad (i.e. i = 2, \dots, N - 1), \\ (ap + u_x)_t - (kp_{\bar{x}}^\sigma)_x = f^\sigma, \quad x = x_i \in \omega_p \setminus \{x_{N-1}\}, \quad t \in \omega_T \quad (i.e. i = 1, \dots, N - 2),$$

$$\begin{aligned}
 (ap + u_x)_t - \frac{k}{h} p_{\bar{x}}^\sigma &= f^\sigma, \quad x = x_{N-1}, \quad t \in \omega_T \quad (i.e. i = N - 1), \\
 p_0 = 0, \quad u_N &= 0, \quad t \in \omega_T, \\
 ap + u_x &= 1, \quad x = x_i \in \bar{\omega}_p, \quad t = 0, \quad (i.e. i = 1, \dots, N - 1),
 \end{aligned} \tag{7}$$

where

$$v_i = v^H(x_i) = \left( \frac{1}{h} \int_{\xi_i}^{\xi_{i+1}} \frac{dx}{v(x)} \right)^{-1}, \quad k_i = k^H(\xi_i) = \left( \frac{1}{h} \int_{x_{i-1}}^{x_i} \frac{dx}{k(x)} \right)^{-1}, \tag{8}$$

$$a_i = a(x_i) = \frac{1}{h} \int_{\xi_i}^{\xi_{i+1}} a(x) dx, \quad f_i(t) = \frac{1}{h} \int_{\xi_i}^{\xi_{i+1}} f(x, t) dx. \tag{9}$$

**2.4. Operator Form of the Difference Scheme**

First we define the discrete divergence operator  $D$

$$\begin{aligned}
 D : H_{\omega_u} \rightarrow H_{\omega_p} : (Du, p)_{\omega_p} &= \sum_{i=1}^{N-2} (u(\xi_{i+1}) - u(\xi_i)) p(x_i) - u(\xi_{N-1}) p(x_{N-1}), \\
 &\qquad \qquad \qquad \forall u \in H_{\omega_u}, \forall p \in H_{\omega_p}
 \end{aligned}$$

and the discrete gradient operator  $G$

$$G : H_{\omega_p} \rightarrow H_{\omega_u} : (Gp, u)_{\omega_u} = p(x_1) u(\xi_1) + \sum_{i=2}^{N-1} (p(x_i) - p(x_{i-1})) u(\xi_i), \quad \forall p \in H_{\omega_p}, \forall u \in H_{\omega_u}.$$

The right-hand sides give rise to bilinear forms on the spaces of discrete functions and define linear operators, which could be expressed in a component form as

$$x_i \in \omega_p : (Du)_i = (Du)(x_i) = \begin{cases} u_{x,i} := (u(\xi_{i+1}) - u(\xi_i))/h, & \text{for } i = 1, \dots, N - 2, \\ -u(\xi_{N-1})/h, & \text{for } i = N - 1. \end{cases} \tag{10}$$

$$\xi_i \in \omega_u : (Gp)_i = (Gp)(\xi_i) = \begin{cases} p(x_1)/h, & \text{for } i = 1, \\ p_{\bar{x},i} := (p(x_i) - p(x_{i-1}))/h, & \text{for } i = 2, \dots, N - 1. \end{cases} \tag{11}$$

Using summation by parts one can easily show that for any discrete functions  $u \in H_{\omega_u}, p \in H_{\omega_p}$ , operators  $G$  and  $D$  are adjoint to each other in the following sense  $(Gp, u)_{\omega_u} = -(p, Du)_{\omega_p}$ .

We also introduce operators that represent multiplication by a scalar grid functions  $a, v$ , and  $k$  defined by (8) and (9) in the spaces  $H_{\omega_p}$  and  $H_{\omega_u}$ :

$$\begin{aligned}
 Q : H_{\omega_p} \rightarrow H_{\omega_p} : \quad a &\in H_{\omega_p}, \quad (Qp, q)_{\omega_p} = (ap, q)_{\omega_p} \quad \forall p, q \in H_{\omega_p}, \\
 N : H_{\omega_p} \rightarrow H_{\omega_p} : \quad v &\in H_{\omega_p}, \quad (Np, q)_{\omega_p} = (vp, q)_{\omega_p}, \quad \forall p, q \in H_{\omega_p}, \\
 K : H_{\omega_u} \rightarrow H_{\omega_u} : \quad k &\in H_{\omega_u}, \quad (Ku, v)_{\omega_u} = (ku, v)_{\omega_u}, \quad \forall u, v \in H_{\omega_u}.
 \end{aligned}$$

Finally, we introduce the operators  $A$  and  $B$ :

$$A: H_{\omega_u} \rightarrow H_{\omega_u}: \quad A = -GND, \quad \text{and} \quad B: H_{\omega_p} \rightarrow H_{\omega_p}: \quad B = -DKG.$$

It is obvious from the definition that that the operators  $A$  and  $B$  are self-adjoint and positive definite in the inner products of the spaces  $H_{\omega_u}$  and  $H_{\omega_p}$ , respectively, and therefore they define new (energy) norms:

$$\|u\|_A = (u, u)_A^{1/2} = (Au, u)_{\omega_u}^{1/2}, \quad \|p\|_B = (p, p)_B^{1/2} = (Bp, p)_{\omega_p}^{1/2}.$$

The discrete operators defined above are invertible, the inverse operators are also self-adjoint and positive definite, and thus they define norms. For the further analysis we will need some properties of the operators and operator norms introduced above. These properties are given in the following lemma.

**Lemma 2.1.** *For any  $v \in H_{\omega_u}$  and  $q \in H_{\omega_p}$  we have*

$$\begin{aligned} \|Dv\|_{\omega_p} &\leq c_v \|v\|_A, & \|Gq\|_{A^{-1}} &\leq c_v \|q\|_{\omega_p}, \\ \|Gq\|_{\omega_u} &\leq c_k \|q\|_B, & \|Dv\|_{B^{-1}} &\leq c_k \|v\|_{\omega_u}, \\ \|q\|_{\omega_p} &\leq \sqrt{2}c_k \|q\|_B, & \|v\|_{\omega_u} &\leq \sqrt{2}c_v \|v\|_A, \end{aligned} \tag{12}$$

where  $c_v = (\min_{x \in \omega_p} \{v(x)\})^{-1/2}$  and  $c_k = (\min_{x \in \omega_p} \{k(x)\})^{-1/2}$ .

**Proof.** The proof of these inequalities follows from the definition of the operators  $D$ ,  $G$ ,  $A$ , and  $B$ . By the definition of the  $A$ -norm of  $v \in H_{\omega_u}$  we have

$$\|v\|_A^2 = (Av, v)_{\omega_u} = (-GNDv, v)_{\omega_u} = (NDv, Dv)_{\omega_p}^{1/2} \geq \min_{x \in \omega_p} \{v(x)\} (Dv, Dv)_{\omega_p},$$

which proves the first inequality. The other inequalities are obtained in the same manner. Note that the last two inequalities follow easily from the above consideration and the discrete analogs of Poincare inequality (see, e.g., [12, p. 110–114]):  $\|q\|_{\omega_p}^2 \leq 2(Gp, Gp)_{\omega_u}$ . ■

Using the above notations, we can write difference scheme (7) in an operator form: find  $u^{j+1} \in H_{\omega_u}$  and  $p^{j+1} \in H_{\omega_p}$  such that

$$\begin{aligned} Au^{j+1} + Gp^{j+1} &= 0, & j &= 0, 1, \dots, M - 1, \\ (Qp^j + Du^j)_t + Bp^\sigma &= f^\sigma, & j &= 0, 1, \dots, M - 1, \\ Qp^0 + Du^0 &= 1, & j &= 0. \end{aligned} \tag{13}$$

For smooth coefficients (e.g., single layered porous media), second-order convergence in operator norms is proven in [9]. In this article we give a theoretical analysis of the convergence rate of the difference scheme (13) in the case of discontinuous coefficients.

**Remark 2.1.** From the above derivation of the scheme and the proofs of various estimates we easily see that the proposed approximations are easily extended to multidimensional rectangular grids and problems with interfaces that are parallel to the grid lines.

**3. ANALYSIS OF THE SCHEME WITH HARMONIC AVERAGING OF THE COEFFICIENTS**

**3.1. Stability of the Finite Difference Scheme**

Studying the scheme for problem with discontinuous coefficients will be done in the framework of the operator theory of finite difference schemes (see, e.g., [12, 14]). The following proposition, is a straightforward reformulation of the similar proposition from [9], establishes the stability of the scheme will be used throughout this article for deriving *a priori* error estimates.

**Proposition 3.1.** *If  $\sigma \geq 0.5$ , then the solution of the difference scheme (13) satisfies the following relation for any  $j \geq 0$ :*

$$\|u^{j+1}\|_A^2 + \|p^{j+1}\|_Q^2 \leq \|u^j\|_A^2 + \|p^j\|_Q^2 + \frac{\tau}{2} \|f^\sigma\|_{B^{-1}}^2. \tag{14}$$

Now we introduce the error in the displacement and the pressure:

$$z^j(x) = u^j(x) - u(x, t_j), \quad x \in \omega_u \quad \text{and} \quad r^j(x) = p^j(x) - p(x, t_j), \quad x \in \omega_p.$$

Obviously, the error functions  $z$  and  $r$  satisfy  $r_0^{j+1} = 0, z_N^{j+1} = 0$  and solve the following finite difference problem:

$$\begin{aligned} Az^{j+1} + Gr^{j+1} &= \psi_1^{j+1}, & j = 0, 1, \dots, M - 1, \\ (Qr^j + Dz^j)_t + Br^\sigma &= \psi_2^{j+1}, & j = 0, 1, \dots, M - 1. \\ Qr^0 + Dz^0 &= \psi_2^0, \end{aligned} \tag{15}$$

where the discrete functions  $\psi_1^{j+1} \in H_{\omega_u}$  and  $\psi_2^{j+1} \in H_{\omega_p}$  are approximation (local truncation) errors for the first and second equations, respectively.

**Lemma 3.1.** *The following presentation of the local truncation error is valid:*

$$\psi_1^{j+1} = G\eta_1^{j+1}, \quad \psi_1^{j+1} \in H_{\omega_u}, \quad \eta_1 \in H_{\omega_p}, \tag{16}$$

with  $\eta_{1,i}^{j+1} = \eta_1^{j+1}(x_i) = v_i u_{\bar{x},i+1}^{j+1} - v(x_i) \frac{\partial u}{\partial x}(x_i, t_{j+1})$ , and

$$\psi_2^{j+1} = D\eta_2^j + \tilde{\psi}_2^{j+1}, \quad \tilde{\psi}_2^{j+1} \in H_{\omega_p}, \quad \eta_2 \in H_{\omega_u}, \tag{17}$$

where

$$\eta_{2,i}^j(\xi_i) = \eta_{2,i}^j = (k_i p_{\bar{x},i}^\sigma - u_{t,i}^j) - \left( k \frac{\partial p}{\partial x} - \frac{\partial u}{\partial t} \right) (\xi_i, t_{j+0.5}), \tag{18}$$

$$\tilde{\psi}_{2,i}^j = a_i p_{i,t}^j - \frac{1}{h} \int_{\xi_i}^{\xi_{i+1}} \frac{\partial}{\partial t} (ap(x, t_{j+0.5})) dx - \left( f_i^\sigma - \frac{1}{h} \int_{\xi_i}^{\xi_{i+1}} f(x, t_{j+0.5}) dx \right). \tag{19}$$

**Proof.** The above representation of the truncation error follows easily from the corresponding “balance” equations. Namely, we take the first equation (3) for  $t = t_{j+1}$  and integrate over one interval of the mesh  $\omega_u$ . Similarly, we take the second equation (3) at  $t = t_{j+(0.5)}$  and integrate over one cell of the mesh  $\omega_p$ . As a result we get (16), (17), (18), and (19). ■

If the coefficients of the problem are smooth, it is easy to show that  $\psi_1^j$  and  $\psi_2^j$  are  $O(h^2 + \tau^{m_\sigma})$ , where  $m_\sigma = 1$  if  $\sigma \neq 0.5$  and  $m_\sigma = 2$  if  $\sigma = 0.5$ . Thus, error estimate follows easily from the stability of the scheme. In the case of interfaces the situation needs more refined analysis. Below, we shall present two cases, arbitrary location of the interface position with respect to grid points and interface at a grid point.

### 3.2. Error Estimate for an Arbitrary Position of the Interface

In this case the parameter  $\theta$  in  $\zeta = \xi_n + \theta h$  can take any value between 0 and 1. Namely, we prove the following.

**Proposition 3.2.** *Assume that the solution  $u(x, t)$  and  $p(x, t)$  of the problem (3) is sufficiently smooth for  $t > 0$  in each of the subintervals  $(0, \zeta)$  and  $(\zeta, 1)$  and  $u^0$  and  $p^0$  are  $O(h^{3/2})$  approximations of  $u(x, 0)$  and  $p(x, 0)$ , respectively. Then the finite difference scheme (13) is convergent and the following a priori error estimate holds:*

$$\|p^j - p(t_j)\|_{\omega_p} + \|u^j - u(t_j)\|_A \leq C(h^{3/2} + \tau^{m_\sigma}), \quad (20)$$

with a constant  $C$  independent of  $h$  and  $\tau$ ,  $m_\sigma = 1$  if  $\sigma > 0.5$ , and  $m_\sigma = 2$  if  $\sigma = 0.5$ .

The proof of the above estimate is quite technical and is done in several steps. In order to improved the readability of the article and to stress on the main results we have moved the proof of this proposition to the Appendix. The same strategy we use for Proposition 3.3.

### 3.3. Error Estimate When the Interface is a Grid Node in $\omega_u$

The results from the previous subsection are valid for an interface position, independently of its location with respect to grid points. A better estimate can be obtained in the particular case when the interface coincides with a node of the grid  $\omega_u$ , i.e.,  $\zeta = \xi_n$  and  $\theta$ , defined in (6), is zero.

**Proposition 3.3.** *Assume that the solution  $u(x, t)$  and  $p(x, t)$  of the problem (3) is sufficiently smooth for  $t > 0$  in each of the subintervals  $(0, \zeta)$  and  $(\zeta, 1)$  and  $u^0$  and  $p^0$  are  $O(h^2)$  approximations of  $u(x, 0)$  and  $p(x, 0)$  respectively, and assume that  $\zeta = \xi_n$ . Then the finite difference scheme (13) is convergent and the following a priori error estimate holds true:*

$$\|p^j - p(t_j)\|_{\omega_p} + \|u^j - u(t_j)\|_A \leq C(h^2 + \tau^{m_\sigma}), \quad (21)$$

with a constant  $C$  independent of  $h$  and  $\tau$ ,  $m_\sigma = 1$  if  $\sigma > 0.5$  and  $m_\sigma = 2$  if  $\sigma = 0.5$ .

## 4. MODIFIED FINITE VOLUME APPROXIMATIONS

Now we will derive two modifications of the scheme, which will allow us to achieve better approximation for both  $W = v \partial_x u$  and  $V = -k \partial_x p$ . Recall, that  $W(x, t)$  in the scheme (7) is approximated by  $w$  at the grid points  $\bar{\omega}_p$  and  $V(x, t)$  by  $v$ , at the grid points  $\bar{\omega}_u$ , where

$$w \in H_{\omega_p} : w = N D u \text{ for } u \in H_{\omega_u}, \quad \text{and} \quad v \in H_{\omega_u} : v = -K G p \text{ for } p \in H_{\omega_p}. \quad (22)$$

**4.1. Finite Difference Scheme with an Improved Approximation of the Stress**

Suppose now that interface position coincides with one of the points  $\omega_p$ , i.e.,  $\zeta = x_n, 1 \leq n \leq N - 1, x_n \in \omega_p$ . To simplify the exposition we shall assume here that  $k$  and  $\nu$  are piecewise constant functions.

Consider the approximation of the flux  $W(x, t)$  using harmonic averaging of the coefficient  $\nu$  at the interface point  $x_n$ :

$$w_n = v_n^H \frac{u_{n+1} - u_n}{h}, \quad \text{where } v_n^H = \frac{2\nu_1\nu_2}{\nu_1 + \nu_2}.$$

Now expand  $u_n$  and  $u_{n+1}$  around  $x_n$ :

$$u_n = u(\zeta - 0, t) - \frac{h}{2}(\partial_x u)^- + \frac{h^2}{8}(\partial_{xx} u)^- - \frac{h^3}{48}(\partial_{xxx} u)^- + O(h^4), \tag{23}$$

$$u_{n+1} = u(\zeta + 0, t) + \frac{h}{2}(\partial_x u)^+ + \frac{h^2}{8}(\partial_{xx} u)^+ + \frac{h^3}{48}(\partial_{xxx} u)^+ + O(h^4), \tag{24}$$

where we have denoted by  $(\partial_x u)^- = \partial_x u(\zeta - 0, t)$ , by  $(\partial_{xx} u)^+ = \partial_{xx} u(\zeta + 0, t)$ , etc.

Now we substitute expansions (23) and (24) into the expression for  $w_n$  and recall that  $u(\zeta - 0, t) = u(\zeta + 0, t)$

$$w_n = \frac{1}{\nu_1 + \nu_2} (\nu_2 \nu_1 (\partial_x u)^- + \nu_1 \nu_2 (\partial_x u)^+) + \frac{h}{4(\nu_1 + \nu_2)} (\nu_1 (\partial_x (\nu_2 \partial_x u))^+ - \nu_2 (\partial_x (\nu_1 \partial_x u))^-) + O(h^2). \tag{25}$$

Next, we use the stress continuity  $\nu_1 (\partial_x u)^- = \nu_2 (\partial_x u)^+ = W$  and rewrite (25) as

$$w_n = W(x_n, t) + \frac{h}{4(\nu_1 + \nu_2)} (\nu_1 (\partial_x W)^+ - \nu_2 (\partial_x W)^-) + O(h^2),$$

from where we get the following approximation for  $W(x_n, t)$ :

$$\tilde{w}_n \equiv v_n^H u_{\bar{x},n+1} - \frac{h}{4} \frac{\nu_1 (\partial_x W)^+ - \nu_2 (\partial_x W)^-}{\nu_1 + \nu_2} = W(x_n, t) + O(h^2). \tag{26}$$

Now taking limits in the first equation of (3) from left and right to the interface we get

$$(\partial_x W)^- = (\partial_x p)^-, \quad (\partial_x W)^+ = (\partial_x p)^+$$

and we rewrite the expression (26) in the form

$$\tilde{w}_n = v_n^H u_{\bar{x},n+1} - \frac{h}{4(\nu_1 + \nu_2)} (\nu_1 (\partial_x p)^+ - \nu_2 (\partial_x p)^-). \tag{27}$$

Using the continuity of the fluid velocity  $k_1 (\partial_x p)^- = k_2 (\partial_x p)^+ = -V$ , and approximating derivatives  $(\partial_x p)^-$  and  $(\partial_x p)^+$  with finite differences  $p_{\bar{x},n}$  and  $p_{\bar{x},n+1}$ , respectively, we obtain the following approximations of the flux

$$\tilde{w}_n^1 = v_n^H u_{\bar{x},n+1} - h \frac{k_1 \frac{\nu_1}{k_2} - \frac{\nu_2}{k_1}}{4 \nu_1 + \nu_2} p_{\bar{x},n}, \quad \tilde{w}_n^2 = v_n^H u_{\bar{x},n+1} - h \frac{k_2 \frac{\nu_1}{k_2} - \frac{\nu_2}{k_1}}{4 \nu_1 + \nu_2} p_{\bar{x},n+1}. \tag{28}$$

Note that  $\tilde{w}_n^1 = W(x_n, t) + O(h^2)$  and  $\tilde{w}_n^2 = W(x_n, t) + O(h^2)$ .

The above discussion results in the following modifications of the scheme (13):

$$\begin{aligned} Au^{j+1} + \tilde{K}Gp^{j+1} &= 0, & j = 0, 1, \dots, M-1, \\ (p^j + Du^j)_t + Bp^\sigma &= f^\sigma, & j = 0, 1, \dots, M-1, \\ Qp^0 + Du^0 &= 1, & j = 0, \end{aligned} \quad (29)$$

where the operator  $\tilde{K} : H_{\omega_u} \rightarrow H_{\omega_u}$  is defined as

$$(\tilde{K}u)_i = \begin{cases} u_i, & \text{for } i \neq n, n+1, \\ \left(1 + \frac{k_1}{4} \frac{\frac{v_1}{k_2} - \frac{v_2}{k_1}}{v_1 + v_2}\right) u_i, & \text{for } i = n, \\ \left(1 - \frac{k_2}{4} \frac{\frac{v_1}{k_2} - \frac{v_2}{k_1}}{v_1 + v_2}\right) u_i, & \text{for } i = n+1. \end{cases} \quad (30)$$

Obviously, the difference between the modified scheme (29) and the scheme (13) is in the approximation of the flux  $W(x, t)$  at the interface point  $x_n$ . As a consequence, the approximation of the first equation of the system (3) has changed in the two neighboring to the interface points,  $\xi_n$  and  $\xi_{n+1}$ . The modified scheme provides a second-order of approximation for both stress and velocity when the interface position coincides with point  $x_n$ .

**Remark 4.1.** The modified scheme is derived supposing that the  $O(h)$  reminder term in (25) is dominating the error. One can easily see from (28), that the above modifications give no improvement in the case when the parameters of the media are such that  $v_1 k_1 = v_2 k_2$ , and they give negligibly small improvement when the following inequalities hold:

$$\left| \frac{1}{4} \frac{v_2 - v_1 \frac{k_1}{k_2}}{v_1 + v_2} \right| \ll 1, \quad \left| \frac{1}{4} \frac{v_2 \frac{k_2}{k_1} - v_1}{v_1 + v_2} \right| \ll 1. \quad (31)$$

## 4.2. Finite Difference Scheme with Improved Approximation of the Velocity

If the interface position coincides with one of the grid points of  $\bar{\omega}_u$ , i.e.  $\zeta = \xi_n$ , where  $1 \leq n \leq N-1$  is some integer, another modification of the scheme (13) can be derived. Analogously to the previous section, we modify expressions, approximating the flux  $V(x, t)$  near the interface by

$$\tilde{v}_n = -k_n^H p_{\bar{x},n} - \frac{h}{4(k_1 + k_2)} \left( k_1 f_n^+ - k_2 f_n^- - k_2 (a_1 p_{n-1} + u_{x,n-1})_t + k_1 \left( a_2 p_{n-1} + \frac{v_1}{v_2} u_{x,n-1} \right)_t \right)$$

or

$$\tilde{v}_n = -k_n^H p_{\bar{x},n} - \frac{h}{4(k_1 + k_2)} \left( k_1 f_n^+ - k_2 f_n^- - k_2 \left( a_1 p_n + \frac{v_2}{v_1} u_{x,n} \right)_t + k_1 (a_2 p_n + u_{x,n})_t \right).$$

According to these modified expressions for the flux, the equations of the (13) are changed just at the points  $i = n-1$  and  $i = n$  so that the operator form of the modified scheme now is

$$\begin{aligned} Au^{j+1} + Gp^{j+1} &= 0, & j = 0, 1, \dots, M-1, \\ (\tilde{Q}p^j + \tilde{N}Du^j)_t + Bp^\sigma &= \tilde{f}^\sigma, & j = 0, 1, \dots, M-1, \\ Qp^0 + Du^0 &= 1, & j = 0. \end{aligned} \quad (32)$$

The operators  $A, G, B,$  and  $D$  were introduced above,  $\tilde{Q} : H_{\omega_p} \rightarrow H_{\omega_p}$  and  $\tilde{N} : H_{\omega_p} \rightarrow H_{\omega_p}$  are defined as

$$(\tilde{Q}p)_i = \begin{cases} a_1 p_i, & \text{for } i = 1, \dots, n - 2, \\ \left( a_1 + \frac{1}{4} \frac{k_1 a_2 - k_2 a_1}{k_1 + k_2} \right) p_i, & \text{for } i = n - 1, \\ \left( a_2 - \frac{1}{4} \frac{k_1 a_2 - k_2 a_1}{k_1 + k_2} \right) p_i, & \text{for } i = n, \\ a_2 p_i, & \text{for } i = n + 1, \dots, N - 1, \end{cases} \tag{33}$$

$$(\tilde{N}q)_i = \begin{cases} q_i, & \text{for } i \neq n - 1, n, \\ \left( 1 + \frac{\nu_1}{4} \frac{\frac{k_1}{\nu_2} - \frac{k_2}{\nu_1}}{k_1 + k_2} \right) q_i, & \text{for } i = n - 1, \\ \left( 1 + \frac{\nu_2}{4} \frac{\frac{k_2}{\nu_1} - \frac{k_1}{\nu_2}}{k_1 + k_2} \right) q_i, & \text{for } i = n, \end{cases} \tag{34}$$

and the modified right hand side  $\tilde{f}$  is

$$\tilde{f}_i = \begin{cases} f_i, & \text{for } i \neq n - 1, n, \\ f_i + \frac{1}{4} \frac{k_1 f_n^+ - k_2 f_n^-}{k_1 + k_2}, & \text{for } i = n - 1, \\ f_i - \frac{1}{4} \frac{k_1 f_n^+ - k_2 f_n^-}{k_1 + k_2}, & \text{for } i = n. \end{cases} \tag{35}$$

Note that the operators  $\tilde{Q}$  and  $\tilde{N}$  are positive. One can develop a similar theory as above and show that the scheme is well posed and gives  $O(h^2)$  convergence rate in energy norm. We shall not elaborate further on this matter.

**Remark 4.2.** One can easily see that these modifications give no improvement when

$$k_1 a_2 = k_2 a_1, \quad k_1 \nu_1 = k_2 \nu_2, \quad k_1 f_n^+ = k_2 f_n^-.$$

In this case the correction terms in corresponding expressions are zero and the scheme is identical to the initial one.

### 5. NUMERICAL EXPERIMENTS

In this section first we present results of numerical experiments, based on the scheme (7), and compute the order of convergence for all unknowns. Then, in four examples we show the numerical results for the stresses, calculated with the scheme (7) and the modified scheme (29).

**Example 1.** In this test the numerical solution is compared to the known exact solution and the relative error in discrete  $L_2$ - and discrete maximum norm (C-norm; see Fig. 2) are calculated:

$$\| \epsilon_w \|_{L_2} = \frac{\sum_{x_i \in \omega_{\tilde{w}}} h |w^{ex}(x_i, t_j) - w_i^{app}|}{\max_{\omega_{\tilde{w}}} |w^{ex}(x_i, t_j)|}, \quad \| \epsilon_w \|_c = \frac{\max_{x_i \in \omega_{\tilde{w}}} |w^{ex}(x_i, t_j) - w_i^{app}|}{\max_{x_i \in \omega_{\tilde{w}}} |w^{ex}(x_i, t_j)|}.$$

Here  $w^{ex}$  and  $w^{app}$  stand for the exact and numerical solutions, respectively, and  $w = \{u, p, V, W\}$ . We take  $\sigma = 0.5$  so that the scheme has second-order accuracy in time.

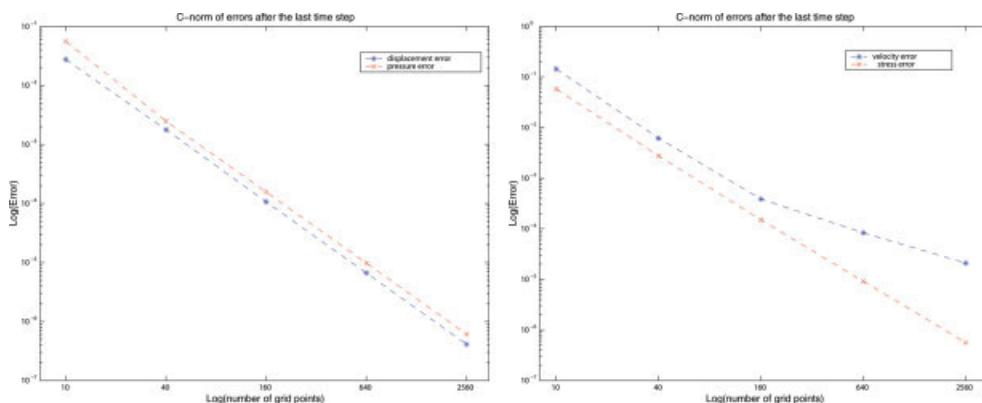


FIG. 2. Example 1: errors for pressure and displacement (left) and velocity and stress (right). [Color figure can be viewed in the online issue, which is available at [www.interscience.wiley.com](http://www.interscience.wiley.com).]

Here we choose

$$\begin{aligned}
 v_1 &= 1, & v_2 &= \tan\left(\frac{1}{12}\right) \tan\left(\frac{10\pi}{3}\right) / (8\pi) \approx 0.0058, \\
 k_1 &= 1, & k_2 &= 1 / \left(8\pi \tan\left(\frac{1}{12}\right) \tan\left(\frac{10\pi}{3}\right)\right) \approx 0.275, \\
 a_1 &= 0, & a_2 &= 0 & \text{and} & f(x, t) = 0.
 \end{aligned}$$

The position of the interface is at  $\zeta = \frac{1}{6}$ . Then an exact solution of the problem (3) with a different initial conditions is

$$\begin{aligned}
 p(x, t) &= \begin{cases} \cos\left(\frac{10\pi}{3}\right) \sin(0.5x)e^{-0.25t}, & x \leq \frac{1}{6}, \\ \sin\left(\frac{1}{12}\right) \cos(4\pi(1-x))e^{-0.25t}, & x > \frac{1}{6}, \end{cases} \\
 u(x, t) &= \begin{cases} -2 \cos\left(\frac{10\pi}{3}\right) \cos(0.5x)e^{-0.25t}, & x \leq \frac{1}{6}, \\ -\frac{2 \cos\left(\frac{1}{12}\right)}{\tan\left(\frac{10\pi}{3}\right)} \sin\left(\frac{1}{12}\right) \sin(4\pi(1-x))e^{-0.25t}, & x > \frac{1}{6}. \end{cases}
 \end{aligned}$$

This solution satisfies interface conditions from (3). The initial conditions are calculated from the above formulae at  $t = 0$ . Analytical expressions for the fluid velocity and for the stress of

TABLE I. Example 1: convergence in  $L_2$ -norm at the time  $t = 0.1$ .

$h = \tau$	$\ \epsilon_u\ _{L_2}$	Ratio	$\ \epsilon_p\ _{L_2}$	Ratio	$\ \epsilon_v\ _{L_2}$	Ratio	$\ \epsilon_w\ _{L_2}$	Ratio
1/10	0.222E-02	—	0.155E+00	—	0.130E+00	—	0.739E-01	—
1/40	0.508E-03	4.4	0.243E-01	6.4	0.153E-01	8.5	0.106E-01	7.0
1/160	0.368E-04	13.8	0.105E-02	23.1	0.789E-03	19.4	0.488E-03	21.7
1/640	0.222E-05	16.6	0.634E-04	16.6	0.639E-04	12.3	0.298E-04	16.4
1/2560	0.137E-06	16.2	0.393E-05	16.1	0.657E-05	9.7	0.185E-05	16.1
Rate	—	2.0	—	2.0	—	1.6	—	2.0

TABLE II. Example 1: convergence in  $L_2$ -norm at the time  $t = 1$ .

$h = \tau$	$\ \epsilon_u\ _{L_2}$	Ratio	$\ \epsilon_p\ _{L_2}$	Ratio	$\ \epsilon_v\ _{L_2}$	Ratio	$\ \epsilon_w\ _{L_2}$	Ratio
1/10	0.276E-01	—	0.559E-01	—	0.737E-01	—	0.273E-01	—
1/40	0.178E-02	15.5	0.248E-02	22.5	0.399E-02	18.5	0.156E-02	17.5
1/160	0.107E-03	16.6	0.157E-03	15.8	0.248E-03	16.1	0.973E-04	16.0
1/640	0.662E-05	16.1	0.977E-05	16.1	0.159E-04	15.6	0.607E-05	16.0
1/2560	0.413E-06	16.1	0.610E-06	16.0	0.110E-05	14.5	0.379E-06	16.0
Rate	—	2.0	—	2.0	—	1.9	—	2.0

the solid are calculated from the Darcy law  $V(x, t) = -k[\partial p(x, t)]/\partial x$  and the stress-strain relationship  $W(x, t) = v[\partial u(x, t)]/\partial x$ , respectively. The resulting formulas are as follows:

$$V(x, t) = \begin{cases} \cos\left(\frac{10\pi}{3}\right) \cos(0.5x)e^{-0.25t}, & x \leq \frac{1}{6}, \\ \frac{\cos\left(\frac{1}{12}\right)}{8\pi \tan\left(\frac{10\pi}{3}\right)} \sin\left(\frac{1}{12}\right) \sin(4\pi(1-x))e^{-0.25t}, & x > \frac{1}{6}, \end{cases}$$

$$W(x, t) = \begin{cases} \cos\left(\frac{10\pi}{3}\right) \sin(0.5x)e^{-0.25t}, & x \leq \frac{1}{6}, \\ \sin\left(\frac{1}{12}\right) \cos(4\pi(1-x))e^{-0.25t}, & x > \frac{1}{6}. \end{cases}$$

Convergence results are summarized in Tables I–IV. Note, that the mesh size  $h$  is decreased in a way, preserving a constant value for the parameter  $\theta$  in the expression  $\zeta = x_{n-0.5} + \theta h$ . The convergence results are given for two time moments,  $t = 0.1$  and  $t = 1.0$ . The rate of convergence is presented in each table in the last line and is calculated according to the following formula:

$$\text{rate} = \frac{\ln \frac{\|\epsilon_1\|}{\|\epsilon_2\|}}{\ln \frac{h_1}{h_2}}, \tag{36}$$

where  $\epsilon_1$  are  $\epsilon_2$  are errors, calculated for grids with step-sizes  $h_1 = 1/640$  and  $h_2 = 1/2560$ , respectively.

Our first observation is that there is no substantial change in the errors monitored at time moments  $t = 0.1$  and  $t = 1.0$ . The existing theoretical error estimates for this problem (see, e.g., [9] for the case of continuous coefficients), predict some increase of the error in time. Our computations show that the theoretical estimates are overestimating the error.

Our second observation is that the displacement, the pressure, and the stress converge with second-order in time and in space both in  $L_2$ - and in maximum norms. The fluid velocity converges with second-order in  $L_2$ -norm and with first order in maximum norm. On very coarse grids velocity converges with higher than first order in maximum norm, a possible reason is that these grids are far from the asymptotic regime. It is known that the space or time truncation error

TABLE III. Example 1: convergence in maximum norm at the time  $t = 0.1$ .

$h = \tau$	$\ \epsilon_u\ _c$	Ratio	$\ \epsilon_p\ _c$	Ratio	$\ \epsilon_v\ _c$	Ratio	$\ \epsilon_w\ _c$	Ratio
1/10	0.518E-02	—	0.226E+00	—	0.322E+00	—	0.196E+00	—
1/40	0.306E-02	16.9	0.304E-01	7.4	0.833E-01	3.9	0.273E-01	7.2
1/160	0.337E-03	9.1	0.139E-02	21.9	0.470E-02	17.7	0.114E-02	23.9
1/640	0.224E-04	15.0	0.841E-04	16.5	0.107E-02	4.4	0.712E-04	16.0
1/2560	0.142E-05	15.8	0.522E-05	16.1	0.262E-03	4.1	0.442E-05	16.1
Rate	—	2.0	—	2.0	—	1.0	—	2.0

TABLE IV. Example 1: convergence in maximum norm at the time  $t = 1$ .

$h = \tau$	$\ \epsilon_u\ _c$	Ratio	$\ \epsilon_p\ _c$	Ratio	$\ \epsilon_v\ _c$	Ratio	$\ \epsilon_w\ _c$	Ratio
1/10	0.645E-01	—	0.963E-01	—	0.145E+00	—	0.581E-01	—
1/40	0.620E-02	10.7	0.481E-02	20.0	0.619E-02	23.4	0.277E-02	21.0
1/160	0.382E-03	16.2	0.284E-03	16.9	0.387E-03	16.0	0.151E-03	18.3
1/640	0.238E-04	16.1	0.174E-04	16.3	0.832E-04	4.7	0.913E-05	16.5
1/2560	0.148E-05	16.1	0.108E-05	16.1	0.210E-04	4.0	0.566E-06	16.1
Rate	—	2.0	—	2.0	—	1.0	—	2.0

terms could dominate and thus could govern the error, depending on the set of space and time discretization parameters used. Tables I–IV also illustrate such a behavior: on the coarse grids the space discretization governs the error for the velocity, while on the finer meshes the time discretization error dominates.

Further, on Figs. 3–5 we compare the stress calculated with the schemes (7) and (29) for three examples. The aim is to illustrate the accuracy of the modified scheme for different sets of the parameters. Solid lines in these figures represent the exact solution obtained on a very fine mesh by the scheme (7). Note that on such grids both schemes, the basic and the modified, give very similar results, which are not distinguishable on these pictures. The advantage of the modified scheme becomes more evident on coarser grids.

**Example 2.** Input data for this test are as follows:  $\zeta = \frac{2}{7}$ ,  $\nu_1 = 1.0$ ,  $\nu_2 = 50.0$ ,  $k_1 = 1.0$ ,  $k_2 = 0.5$ ,  $a = 0$ . Comparison results at the time  $t = 0.05$  are shown in Fig. 3. We see that coarse grid solutions calculated with both schemes differ from the fine grid solution; however, the modified scheme provides a better approximation.

**Example 3.** In this experiment we choose following input parameters:  $\zeta = \frac{2}{3}$ ,  $\nu_1 = 1.0$ ,  $\nu_2 = 0.01$ ,  $k_1 = 1.0$ ,  $k_2 = 0.1$ ,  $a = 0$ ,  $t = 1.0$ . Figure 4 shows that the modified scheme gives

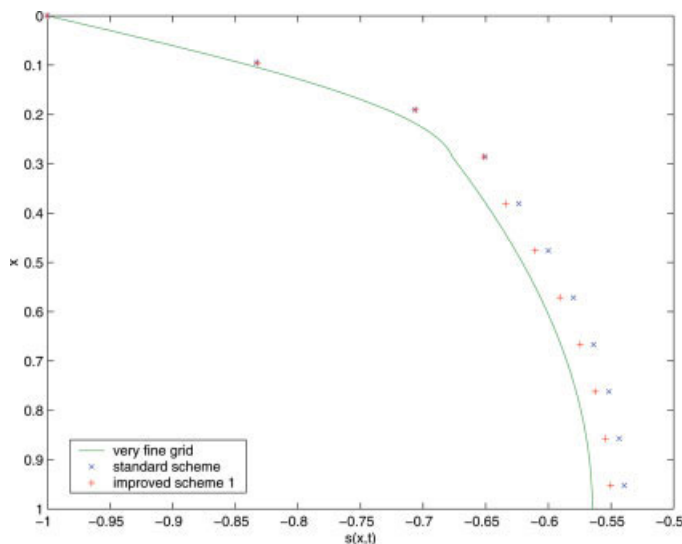


FIG. 3. The stress for Example 2. [Color figure can be viewed in the online issue, which is available at [www.interscience.wiley.com](http://www.interscience.wiley.com).]

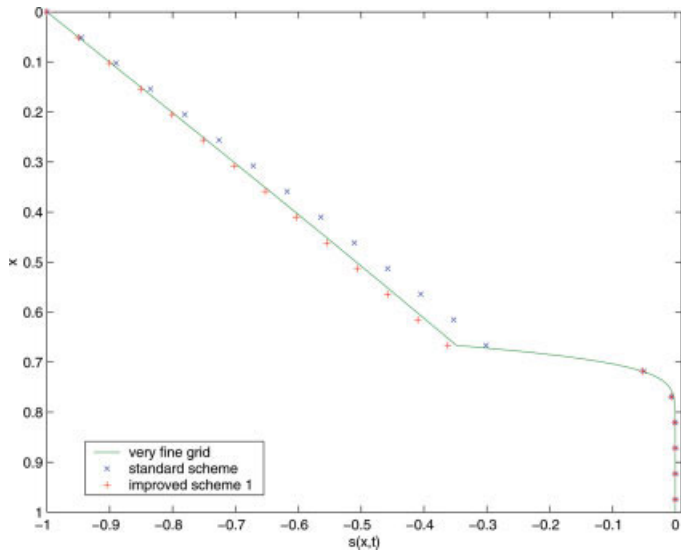


FIG. 4. The stress for Example 3. [Color figure can be viewed in the online issue, which is available at [www.interscience.wiley.com](http://www.interscience.wiley.com).]

very good approximation to the solution even on relatively coarse grids, which is not the case for the standard (not modified) scheme.

**Example 4.** Here we take  $\zeta = \frac{2}{3}$ ,  $\nu_1 = 1.0$ ,  $\nu_2 = 0.1$ ,  $k_1 = 1.0$ ,  $k_2 = 9.0$ ,  $a = 0$ ,  $t = 0.1$ . For these parameters the both schemes give almost identical results (see Fig. 5) that is in accordance with Remark 4.1.

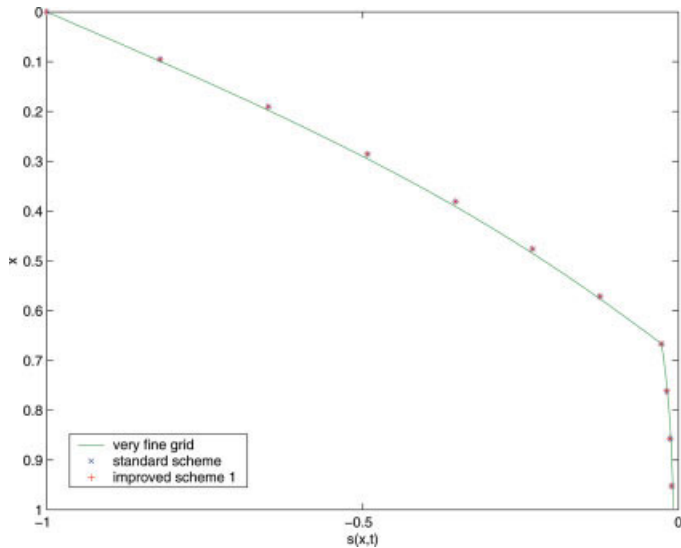


FIG. 5. The stress for Example 4. [Color figure can be viewed in the online issue, which is available at [www.interscience.wiley.com](http://www.interscience.wiley.com).]

6. APPENDIX

**Proof of Proposition 3.2.** The first step will be to establish estimates for the errors  $z$  and  $r$ , introduced in (15). For any fixed  $j$  we split displacement error  $z = z^j$  in the following way:

$$z = z_1 + z_2, \quad \text{where} \quad Az_1 = \psi_1. \tag{37}$$

Then using this and the equation  $Az_{1,t} = \psi_{1,t}$  we get

$$\|z_1\|_A = \|\psi_1\|_{A^{-1}}, \quad \text{and} \quad \|z_{1,t}\|_A \leq C\|\psi_{1,t}\|_{A^{-1}}. \tag{38}$$

Since the approximation error  $\psi_1$  can be represented in a form (16), from Lemma 2.1 we have  $\|\psi_1\|_{A^{-1}} \leq c_v\|\eta_1\|_{\omega_p}$ . Using Taylor expansion we easily see that  $\eta_{1,i} = O(h^2)$  for all  $i \neq n$ , and  $\eta_{1,n} = O(h)$ , so  $\|\eta_1\|_{\omega_p} = O(h^{3/2})$ . Similar estimates are valid for the discrete time derivatives of  $\eta$ . Hence, from (38) it follows

$$\|z_1\|_A \leq \|\psi_1\|_{A^{-1}} = O(h^{3/2}) \quad \text{and} \quad \|z_{1,t}\|_A \leq C\|\psi_{1,t}\|_{A^{-1}} = O(h^{3/2}). \tag{39}$$

Consider now the problems for  $r^j$  and  $z_2^j$

$$\begin{aligned} Az_2^{j+1} + Gr^{j+1} &= 0, \quad j = 0, 1, \dots, M-1, \\ (Qr^j + Dz_2^j)_t + Br^\sigma &= \psi_2^{j+1} - Dz_{1,t}^j, \quad j = 0, 1, \dots, M-1 \end{aligned} \tag{40}$$

If  $\sigma \geq 0.5$ , it follows from (14):

$$\|z_2^{j+1}\|_A^2 + \|r^{j+1}\|_Q^2 \leq \|z_2^0\|_A^2 + \|r^0\|_Q^2 + \frac{\tau}{2} \sum_{k=0}^j (\|\psi_2^{k+1}\|_{B^{-1}}^2 + \|Dz_{1,t}^k\|_{B^{-1}}^2), \tag{41}$$

$j = 0, \dots, M-1.$

Consider local truncation error  $\psi_2$ . It can be represented in the form (17), (18), where for  $\theta \leq 0.5$

$$\begin{aligned} \eta_{2,i} &= O(h^2 + \tau^{m\sigma}) & \text{if } i \neq n, \\ \eta_{2,i} &= O(h + \tau^{m\sigma}) & \text{if } i = n, \end{aligned}$$

and for  $\theta > 0.5$

$$\begin{aligned} \eta_{2,i} &= O(h^2 + \tau^{m\sigma}) & \text{if } i \neq n+1, \\ \eta_{2,i} &= O(h + \tau^{m\sigma}) & \text{if } i = n+1. \end{aligned}$$

Furthermore, from (19) one can see that  $\tilde{\psi}_2 = O(h^2 + \tau^{m\sigma})$ .

Then the estimate  $\|\psi_2\|_{\omega_p} \leq \sqrt{2}c_k\|\tilde{\psi}_2\|_B$  of Lemma 2.1 produces  $\|\tilde{\psi}_2\|_{B^{-1}} \leq \sqrt{2}c_k\|\tilde{\psi}_2\|_{\omega_p}$  and taking into account the estimates for  $\eta_2$  and  $\tilde{\psi}_2$  we get

$$\|\psi_2\|_{B^{-1}} \leq \sqrt{2}c_k(\|\eta_2\|_{\omega_u} + \|\tilde{\psi}_2\|_{\omega_p}) = O(\tau^{m\sigma} + h^{3/2}). \tag{42}$$

Next, apply the inequalities of Lemma 2.1 get  $\|Dz_{1,t}\|_{B^{-1}} \leq 2c_k c_v \|z_{1,t}\|_A$ . Further, recall (39) to so that

$$\|Dz_{1,t}\|_{B^{-1}} \leq O(h^{3/2}) \tag{43}$$

and after substitution of (43) into (41) we obtain

$$\|z_2^{j+1}\|_A^2 + \|r^{j+1}\|_Q^2 \leq \|z_2^0\|_A^2 + \|r^0\|_Q^2 + \frac{\tau}{2} \sum_{k=0}^j \left( \|\psi_2^{k+1}\|_{B^{-1}}^2 + c_k c_v \sum_{k=0}^j \|\psi_{1,t}^k\|_{A^{-1}}^2 \right). \tag{44}$$

Finally, since (39) and (42) are valid, from (44) we conclude that  $\|z_2\|_A + \|r\|_Q = O(h^{3/2} + \tau^{m\sigma})$ . Since the operator  $Q$  is essentially a multiplication by a diagonal matrix, it follows  $\|r\|_{\omega_p} = O(h^{3/2} + \tau^{m\sigma})$ . Furthermore, using (39) we have  $\|z\|_A \leq \|z_1\|_A + \|z_2\|_A = O(h^{3/2} + \tau^{m\sigma})$ . So, we proved convergence of the pressure in the discrete  $L_2$ -norm and convergence of the displacement in  $A$ -norm. ■

**Proof of Proposition 3.3.** Consider the local truncation error of the first equation of the system. Since (16) is valid and since in the case when  $\theta = 0$ ,  $\eta_{1,i} = O(h^2)$  for all  $i$ , we have  $\|\psi_1\|_{A^{-1}} \leq \|\eta_1\|_{\omega_p} = O(h^2)$ . Thus, if we split  $z = z_1 + z_2$ , where  $Az_1 = \psi_1$ , then we have

$$\|z_1\|_A \leq C\|\psi_1\|_{A^{-1}} = O(h^2).$$

By taking into account the equation  $Az_{1,t} = \psi_{1,t}$ , one gets in a similar manner the estimate  $\|z_{1,t}\|_A \leq C\|\psi_{1,t}\|_{A^{-1}} = O(h^2)$ .

Now we consider the local truncation error  $\psi_2$ . As before, we split  $\psi_{2,i}$  into two parts according to the formula (17) with  $\tilde{\psi}_2 = O(h^2 + \tau^{m\sigma})$ . A better convergence rate can be obtained largely due to the fact that for  $x = x_i \in \omega_p$

$$(D\eta_2)_i = \begin{cases} O(h^2 + \tau^{m\sigma}) & \text{for } i \neq n - 1, n \\ \frac{\eta_{2,n}}{h} + O(h + \tau^{m\sigma}) & \text{for } i = n - 1, \\ -\frac{\eta_{2,n}}{h} + O(h + \tau^{m\sigma}) & \text{for } i = n, \end{cases}$$

where  $\eta_{2,n} = O(h + \tau^{m\sigma})$ . This indicates that the local truncation error near the interface is essentially  $O(1)$ , but due to its particular form we can still prove second-order convergence.

We proceed in several steps. We first decouple the problem (40). Since  $A = -GND$ , from the first equation we have  $Dz_2 = N^{-1}r$ . After substitution  $Dz_2$  into the second equation of (40) we obtain a problem for the pressure error  $r$  only:

$$(Q + N^{-1})r_t + Br^\sigma = \psi_2 - Dz_{1,t}. \tag{45}$$

Note that  $Q + N^{-1}$  is an operator with a diagonal matrix.

In order to get an optimal order error estimate we split the local truncation error near the interface. Thus, we split  $\psi_2 = \psi_2^* + \psi_2^{**}$ , where

$$\psi_{2,i}^* = \begin{cases} \eta_{2,n}/h, & \text{for } i = n - 1, \\ -\eta_{2,n}/h, & \text{for } i = n, \\ 0, & \text{for } i \neq n - 1, n \end{cases} \quad \text{and} \quad \psi_{2,i}^{**} = O(h^2 + \tau^{m\sigma}) \forall i. \tag{46}$$

Based on this splitting we present the error for the pressure in the form  $r = r_1 + r_2$ , where  $r_1$  and  $r_2$  are solutions of the following problems, respectively

$$(Q + N^{-1})r_{1,t} + Br_1^\sigma = \psi_2^{**} - Dz_{1,t}, \tag{47}$$

$$(Q + N^{-1})r_{2,t} + Br_2^\sigma = \psi_2^*. \tag{48}$$

For  $\sigma \geq 0.5$  the solution of the problem (47) can be estimated as (see, e.g., [12])

$$\|r_1^{j+1}\|_{\omega_p} \leq \|r_1^0\|_{\omega_p} + \sum_{j'=1}^j \tau \|\psi_2^{**j'} - Dz_1^{j'}\|_{\omega_p} \leq \|r_1^0\|_{\omega_p} + \tau \sum_{j'=1}^j (\|\psi_2^{**j'}\|_{\omega_p} + \|Dz_1^{j'}\|_{\omega_p}).$$

To estimate  $Dz_{1,t}$  we use Lemma 2.1 and the fact  $\|z_{1,t}\|_A = O(h^2)$ . Then combining all these we get

$$\|r_1^{j+1}\|_{\omega_p} = O(h^2 + \tau^{m\sigma}). \tag{49}$$

Consider now the problem (48). In view of (46) we can write down  $\psi_2^* = (\eta_2^*)_x$ , where the grid function  $\eta_2^*$  is defined on  $\bar{\omega}_u$  as

$$\eta_{2,i}^* = \begin{cases} 0 = 0, & i = 0, \dots, n - 2, \\ h\psi_{2,n-1}^* = \eta_{2,n}, & i = n - 1, \\ h(\psi_{2,n-1}^* + \psi_{2,n}^*) = 0, & i = n, \dots, N - 1. \end{cases}$$

Using the identity  $r_2^\sigma = r_2 + \sigma \tau r_{2,t}$  and applying the operator  $B^{-1}$  to (48), we rewrite this problem as

$$(B^{-1}(Q + N^{-1}) + \sigma \tau E)r_{2,t} + r_2 = B^{-1}\psi_2^*. \tag{50}$$

Operators  $B^{-1}$  and  $N^{-1}$  are positive definite,  $Q$  is non-negative, hence  $B^{-1}(Q + N^{-1})$  is positive definite, and for  $\sigma \geq 0.5$  the following inequality holds

$$B^{-1}(Q + N^{-1}) + \sigma \tau E \geq \frac{\tau}{2}E.$$

In this case we can write an estimate (see, e.g. [12]) for the solution of the problem (50):

$$\|r_2^{j+1}\|_{\omega_p} \leq \|B^{-1}\psi_2^{*0}\|_{\omega_p} + \|B^{-1}\psi_2^{*j}\|_{\omega_p} + \sum_{j'=1}^j \tau \|B^{-1}\psi_{2,t}^{*j'}\|_{\omega_p}. \tag{51}$$

Here  $\|B^{-1}\psi_2^{*j}\|_{\omega_p}$  can be estimated as (see [12])

$$\|B^{-1}\psi_2^{*j}\|_{\omega_p} \leq c(1, |\eta_2^*|)_{\bar{\omega}_u} = ch|\eta_{2,n}| = O(h^2), \tag{52}$$

where  $c$  is a constant independent on discretization parameters.

It follows from (51):  $\|r_2^{j+1}\|_{\omega_p} = O(h^2 + \tau^{m\sigma})$ . Using this and (49) we get an estimate for the pressure error

$$\|r\|_{\omega_p} \leq \|r_1\|_{\omega_p} + \|r_2\|_{\omega_p} = O(h^2 + \tau^{m\sigma}).$$

To complete the proof, it remains to bound  $\|z_2\|_A$ . Multiplying the first equation of (40) by  $z_2$ , we obtain:

$$\|z_2\|_A^2 = -(Gr, z_2)_{\omega_u}.$$

Taking into account that  $(Gr, z_2)_{\omega_u} = -(r, Dz_2)_{\omega_p}$  and then applying  $\epsilon$ -inequality and Lemma 2.1 we get

$$\|z_2\|_A^2 \leq \epsilon \|r\|_{\omega_p}^2 + \frac{1}{4\epsilon} \|Dz_2\|_{\omega_p}^2 \leq \epsilon \|r\|_{\omega_p}^2 + \frac{c_v^2}{4\epsilon} \|z_2\|_A^2, \quad \epsilon > 0.$$

Choosing  $\epsilon$  properly we kick back the term  $\|r\|_{\omega_p}^2$  so that  $\|z_2\|_A = O(h^2 + \tau^{m\sigma})$ . This yields

$$\|z\|_A \leq \|z_1\|_A + \|z_2\|_A = O(h^2 + \tau^{m\sigma})$$

and concludes the proof. ■

The authors are grateful to the anonymous reviewers for the remarks that helped to improve the presentation. R. Lazarov thanks ITWM and Fraunhofer Society for the hospitality and the financial support during his sabbatical leave when this work was completed.

## References

1. M. Biot, General theory of three dimensional consolidation, J Appl Phys 12 (1941), 155–169.
2. J. Bear and Y. Bachamat, Introduction to modelling of transport Phenomena in Porous Media, Kluwer Academic, Dordrecht, 1990.
3. R. W. Lewis and B. A. Schrefler, The finite element method in the static and dynamic deformation and consolidation of porous media, John Wiley, Chichester, 1998.
4. R. E. Showalter, Diffusion in poroelastic media, J Math Anal Appl 251 (2000), 310–340.
5. S. Jourine, P. P. Valko, and A. K. Kronenberg, Modelling poroelastic cylinder experiments with realistic boundary conditions, Int J Numer Anal Meth Geomech 28 (2004), 1189–1205.
6. H. F. Wang, Theory of linear poroelasticity with application to geomechanics and hydrogeology, Princeton University Press, Princeton, 2000.
7. J. Korsawe and G. Starke, A Least-Squares mixed finite element method for Biot's consolidation problem in porous media, SIAM J Numer Anal 43(1) (2005), 318–339.
8. K. Lipnikov, Numerical methods for the Biot model in poroelasticity, Phd. Thesis, Department of Mathematics, University of Houston, 2002, 116 p.
9. F. J. Gaspar, F. J. Lisbona, and P. N. Vabischevich, A finite difference analysis of Biot's consolidation model, Appl Numer Math 44 (2003), 487–506.
10. F. J. Gaspar, F. J. Lisbona, and P. N. Vabischevich, A numerical model for radial flow through porous and deformable shells, Comput Methods Appl Math 4(1) (2004), 34–47.
11. A. Naumovich, O. Iliev, F. Gaspar, F. Lisbona, and P. Vabishchevich, On numerical solution of 1D poroelasticity equations in a multilayered domain, Math Model Anal 10(3) (2005), 287–304.
12. A. A. Samarskii, Theory of difference schemes, Pure and Applied Mathematics, Marcel Dekker, New York, 2001, 761p.
13. R. E. Ewing, O. P. Iliev, and R. D. Lazarov, A modified finite volume approximation of second-order elliptic equations with discontinuous coefficients, SIAM J Sci Comp 23(4) (2001), 1334–1350.
14. A. A. Samarskii, P. N. Vabischevich, and P. P. Matus, Difference schemes with operator factors, Minsk, 1998, 442p.